

Colloidal Synthesis of Cubic-Phase Copper Selenide Nanodiscs and Their Optoelectronic Properties

Jaewon Choi,[†] Narae Kang,[†] Hye Yun Yang,[†]
Hae Jin Kim,[‡] and Seung Uk Son^{*†}

[†]Department of Chemistry and Department of Energy Science, Sungkyunkwan University, Suwon 440-746, Korea, and [‡]Korea Basic Science Institute, Daejeon 335-333, Korea

Received March 30, 2010

Revised Manuscript Received May 12, 2010

Recently, diverse colloidal semiconductor nanomaterials have been prepared for energy device applications via wet chemical routes.¹ Especially, diverse metal chalcogenides nanomaterials have been extensively studied over the world.² Compared with physical synthetic methods for fabrication of semiconductor films such as chemical vapor deposition, a solution-based approach is favorable for large-area fabrication of devices.

Typically, in colloidal synthesis of metal selenide nanomaterials, mixing insoluble selenium powder with trialkylphosphine forms soluble phosphine selenide, as a common selenium source for use in organic media.³ (Figure 1b) Although trialkylphosphines have been frequently used in the synthesis of nanomaterials as a surfactant, our group often suffered from the uncontrollable shape or size of nanomaterials in the presence of phosphine (even with a little amount).⁴ In addition, phosphines are relatively expensive, toxic to living organisms and sensitive to oxygen forming phosphine oxide.⁵ Thus, new selenium sources without the use of phosphines are required.

Recently, *N*-heterocyclic carbene (NHC) chemistry has attracted a great attention of scientists in organometallics.⁶ By treating imidazolium salts with a base, the carbene species in Figure 1a can be generated. Actually, chemistry of NHC is very similar with that of phosphines.⁶ For example, these carbenes can react with selenium powder to form imidazoline-2-selenone. (Figure 1a) We speculated that this compound

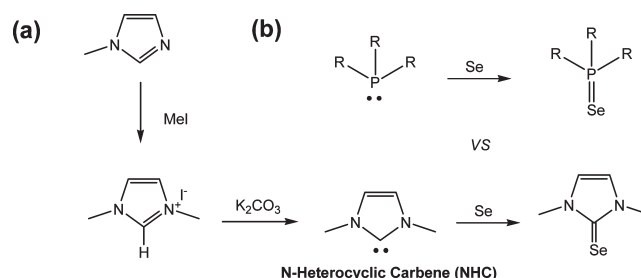


Figure 1. Comparison of chemistry of selenium sources: (a) imidazoline-2-selenone and (b) phosphine selenide.

can function as a selenium source like phosphine selenide in the synthesis of metal selenide nanomaterials. Our research group has focused on the synthesis of colloidal 2D nanomaterials.⁷ In this work, we report the colloidal synthesis of good-quality cubic phase copper selenide nanodiscs using imidazoline-2-selenone and their promising optoelectronic properties.

It has been well-documented that the copper selenides have diverse stoichiometric (CuSe , CuSe_2 , etc) and non-stoichiometric (Cu_{2-x}Se) phases.⁸ The major materials are hexagonal CuSe and cubic Cu_{2-x}Se , which have very promising physical properties for application toward diverse optoelectronic devices such as solar cells.⁸ The phases of copper selenides can be easily distinguished by the powder X-ray diffraction pattern. Although the 2D morphologies of hexagonal CuSe have been reported, it is relatively rare to observe 2D morphologies of cubic Cu_{2-x}Se .¹⁰ Interestingly, in the case of copper sulfide, the synthetic routes for hexagonal (not cubic) phased Cu_2S nanodiscs have been well-documented.¹¹

For synthesis of copper selenide nanodiscs, a new selenium source, air-stable 1,3-dimethylimidazoline-2-selenone was prepared. *N*-Methylimidazole was treated with methyl iodide to form 1,3-dimethylimidazolium iodide salt, which was further treated with potassium carbonate and reacted with selenium powder to form 1,3-dimethylimidazoline-2-selenone¹² (Figure 1a). Using this compound as a selenium source, we screened diverse reaction conditions including solvent, temperature, and amount of reagents to prepare good-quality copper selenide nanomaterials.

In the optimized synthetic procedure for nanodiscs, imidazoline-2-selenone (65 mg, 0.37 mmol) was dissolved

*Corresponding author. E-Mail: sson@skku.edu.

- (1) Talapin, D. V.; Lee, J.-S.; Kovalenko, M. V.; Shevchenko, E. V. *Chem. Rev.* **2010**, *110*, 389.
- (2) (a) Gur, I.; Fromer, N. A.; Geier, M. L.; Alivisatos, A. P. *Science* **2005**, *310*, 462. (b) Ma, W.; Luther, J. M.; Zheng, H.; Wu, Y.; Alivisatos, A. P. *Nano Lett.* **2009**, *9*, 2072. (c) Arango, A. C.; Oertel, D. C.; Xu, Y.; Bawendi, M. G.; Bulovic, V. *Nano Lett.* **2009**, *9*, 860.
- (3) (a) Murray, C. B.; Norris, D. J.; Bawendi, M. G. *J. Am. Chem. Soc.* **1993**, *115*, 8706. (b) Peng, X.; Manna, L.; Yang, W.; Wickham, J.; Scher, E.; Kadavanich, A.; Alivisatos, A. P. *Nature* **2000**, *404*, 59.
- (4) See the example of TEM images in the Supporting Information.
- (5) Fluck, E. *Top. Curr. Chem.* **1973**, *35*, 64.
- (6) (a) Marion, N.; Nolan, S. P. *Acc. Chem. Res.* **2008**, *41*, 1440. (b) Herrmann, W. A. *Angew. Chem., Int. Ed.* **2002**, *41*, 1290.
- (7) (a) Jang, K.; Kim, H. J.; Son, S. U. *Chem. Mater.* **2010**, *22*, 1273. (b) Xu, J.; Jang, K.; Jung, I. G.; Kim, H. J.; Oh, D.-H.; Ahn, J. R.; Son, S. U. *Chem. Mater.* **2009**, *21*, 4347. (c) Park, K. H.; Choi, J.; Kim, H. J.; Oh, D.-H.; Ahn, J. R.; Son, S. U. *Small* **2008**, *4*, 945. (c) Park, K. H.; Jang, K.; Son, S. U. *Angew. Chem., Int. Ed.* **2006**, *45*, 4608.

- (8) Zhang, S.-Y.; Fang, C.-X.; Tian, Y.-P.; Zhu, K.-R.; Jin, B.-K.; Shen, Y.-H.; Yang, J.-X. *Cryst. Growth Des.* **2006**, *6*, 2809, and references therein.
- (9) Malik, M. A.; O'Brien, P.; Revaprasadu, N. *Adv. Mater.* **1999**, *11*, 1441.
- (10) Deng, Z.; Mansuripur, M.; Muscat, A. J. *J. Mater. Chem.* **2009**, *19*, 6201.
- (11) Sigman, M. B.; Ghezelbash, A.; Hanrath, T.; Saunders, A. E.; Lee, F.; Korgel, B. A. *J. Am. Chem. Soc.* **2003**, *125*, 16050.
- (12) (a) Benac, B. L.; Burgess, E. M.; Arduengo, A. J., III. *Organic Synthesis* **1986**, *64*, 92. (b) Choi, J.; Ko, J. H.; Jung, I. G.; Yang, H. Y.; Ko, K. C.; Lee, J. Y.; Lee, S. M.; Kim, H. J.; Nam, J. H.; Ahn, J. R.; Son, S. U. *Chem. Mater.* **2009**, *21*, 2571.

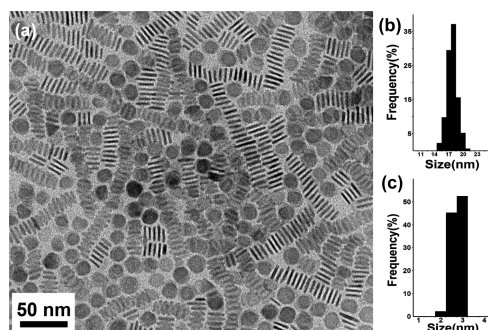


Figure 2. (a) TEM image of the prepared Cu_{2-x}Se nanodiscs; (b) diameter and (c) thickness distribution diagrams by investigating 324 and 347 discs, respectively.

in a mixture of methylene chloride (4 mL) and oleylamine (2 mL). Copper(II) chloride (0.10 g, 0.74 mmol) was dissolved in oleylamine (5 mL) and heated to 175 °C, followed by injection of the imidazoline-2-selenone solution. The subsequent dark brown reaction mixture was stirred for additional 10 min. The solution was then cooled to room temperature. Excess methanol was added to induce precipitation of the nanomaterials, which were retrieved by centrifugation.¹³

Figure 2a shows the representative transmission electron microscopy (TEM) image of the obtained nanomaterials. The top view was circular while the side view of the materials was observed through the columnar assembly of nanodiscs. From TEM studies, the average diameter and thickness were calculated as 17 ± 1 nm and 2.6 ± 0.9 nm respectively (Figure 2b and 2c). Although micro or submicro Cu_{2-x}Se plates have been reported very recently, the diameter size of the reported plates was in the range of 1.0–2.5 μm or 200–300 nm with a thickness range of 12–30 nm.¹⁰ As far as we are aware, the observed diameter and thickness of nanodiscs in this study are smallest of the known 2D Cu_{2-x}Se (vide infra) nanomaterials.

The powder X-ray diffraction (XRPD) and electron diffraction (ED) patterns in Figure 3b and Figure S3 in the Supporting Information clearly support that the phase of copper selenide is cubic Cu_{2-x}Se ¹⁴ (JCPDS #06–0680). The energy dispersive X-ray absorption spectroscopy (EDX) showed a 1.85 average atomic ratio of Cu to Se. (Figure 3a)¹⁵ The X-ray photoelectron spectroscopy (XPS) also supports the Cu_{2-x}Se phase with the copper $2p_{3/2}$ and selenium 3d peaks at 932.2 and 54.0 eV, respectively. (Figure 3c)¹⁶

The nanodiscs were further investigated by high-resolution TEM. As shown in Figure 4, (111) crystal planes with a

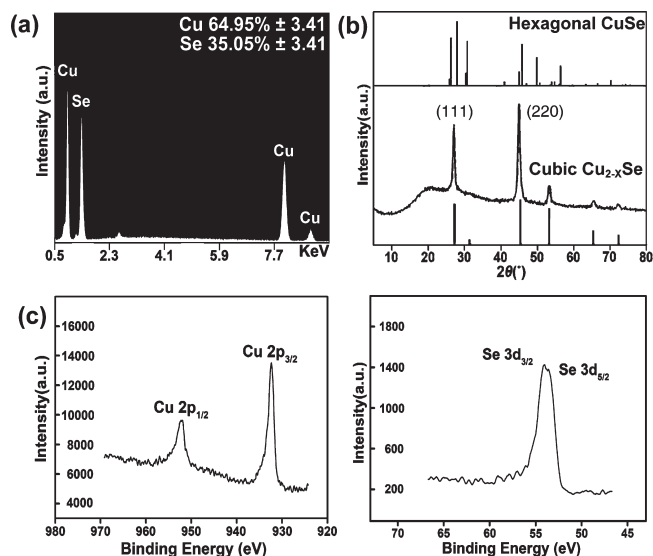


Figure 3. (a) Energy-dispersive X-ray absorption spectroscopy; (b) powder X-ray diffraction patterns; (c) X-ray photoelectron spectroscopy of Cu_{2-x}Se nanodiscs.

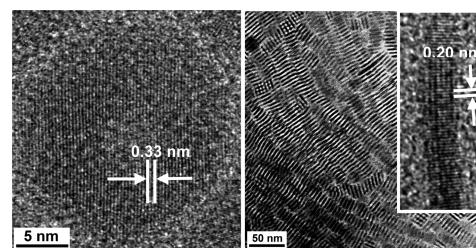


Figure 4. HR-TEM images of the prepared Cu_{2-x}Se nanodiscs.

0.330 nm interplane-distance were observed dominantly. In the side view of nanodiscs, the observed average distance between the crystal planes was 0.204 nm, which corresponds to (220) planes. It is noteworthy that the (111) and (220) planes were dominant in the XRPD pattern.

Although it is not common, a significant number of cubic phase 2D metallic nanomaterials have been known in wet chemical synthesis.¹⁷ Formation of the 2D shape of cubic phased nanomaterials has been traditionally suggested as the result of kinetically controlled crystal growth by ligands. Similarly, the 2D shape evolution of cubic Cu_{2-x}Se has been suggested as the result of the selective interaction of ligands with crystal planes in the growth of nanomaterials.¹⁰ It is noteworthy that *N*-heterocyclic carbenes generated from imidazoline-2-selenone through backward reaction of Figure 1a are excellent coordination ligands like electron rich phosphines for a variety of transition metals. Especially, diverse NHC-copper species were characterized.¹⁸ Thus, we suggest that NHC and oleylamine may play a cooperative role in the shape-controlled synthesis of nanodiscs via interaction with copper on a crystal plane

(13) Following this procedure, nanodiscs with nearly the same quality were prepared reproducibly at least 26 times in our lab for further studies.

(14) (a) Xu, J.; Zhang, W.; Yang, Z.; Ding, S.; Zeng, C.; Chen, L.; Wang, Q.; Yang, S. *Adv. Funct. Mater.* **2009**, *19*, 1759. (b) Cao, H.; Qian, X.; Zai, J.; Yin, J.; Zhu, Z. *Chem. Commun.* **2006**, 4548. (c) Yu, R.; Ren, T.; Sun, K.; Feng, Z.; Li, G.; Li, C. *J. Phys. Chem. C* **2009**, *113*, 10833. (d) Hsu, Y.-J.; Hung, C.-M.; Lin, Y.-F.; Liaw, B.-J.; Lobana, T. S.; Lu, S.-Y.; Liu, C. W. *Chem. Mater.* **2006**, *18*, 3323.

(15) The common X range of the known Cu_{2-x}Se materials is 0–0.25 in ref 14.

(16) Xie, Y.; Zheng, X.; Jiang, X.; Lu, J.; Zhu, L. *Inorg. Chem.* **2002**, *41*, 387.

(17) (a) Puentes, V. F.; Zanchet, D.; Erdonmez, C. K.; Alivisatos, A. P. *J. Am. Chem. Soc.* **2002**, *124*, 12874. (b) Chen, S.; Carroll, D. L. *J. Phys. Chem. B* **2004**, *108*, 5500. (c) Sun, X.; Dong, S.; Wang, E. *Angew. Chem., Int. Ed.* **2004**, *43*, 6360.

(18) (a) Diez-González, S.; Stevens, E. D.; Nolan, S. P. *Chem. Commun.* **2008**, 4747. (b) Jurkauskas, V.; Sadighi, J. P.; Buchwald, S. L. *Org. Lett.* **2003**, *5*, 2417.

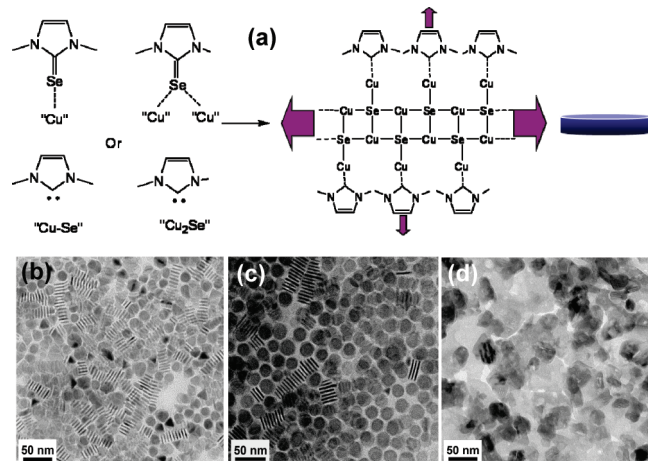


Figure 5. (a) Suggested formation process of nanodiscs; TEM images of nanomaterials prepared by changing the quantity of selenium sources: (b) 0.25; (c) 0.50; (d) 1.0 equiv. of imidazoline-2-selenone to copper sources.

(Figure 5a). When Se powder was used instead of imidazoline-2-selenone under identical experimental conditions, irregularly shaped copper selenide nanomaterials were obtained with contamination of the selenium powder. When the same equivalent trioctylphosphine selenide was used instead of imidazoline-2-selenone, small materials (undetectable by TEM) were obtained.¹⁹

The shape-controlled formation of Cu_{2-x}Se nanodiscs was quite dependent upon concentration of imidazoline-2-selenone. When the equivalent of the selenone was less than 0.5 equiv., tetragonal-shaped materials were mixed. When the equivalent of selenone exceeded 1 equiv., irregularly shaped nanomaterials were formed, unsuitable for dispersion in organic solvents for further studies. (Figure 5b–d)

Recently, frontier research has emerged regarding the photovoltaic application of colloidal nanoparticles.² Although these works focused on cadmium or lead chalcogenides, cadmium and lead are nonetheless, toxic metals.² Recently, environmental-friendly metal chalcogenides such as copper sulfide have been applied toward photovoltaic devices.²⁰

Cu_{2-x}Se is a p-type semiconductor having a ca. 2.2 eV direct bandgap and 1.0–1.4 eV indirect band gap.¹³ It was reported that the indirect band gap was suitable for use as a light absorption layer in solar cell devices.²¹ Figure 6a shows the UV/vis absorption spectrum of Cu_{2-x}Se nanodiscs.¹³ The optical band gap of nanodiscs was estimated to be ca. 1.55 eV by plotting $(\alpha h\nu)^{1/2} = (1/l)^{1/2} (A h\nu)^{1/2}$ versus $h\nu$, in which α , A , l , ν , and h are absorption coefficient, absorbance, light pathway, frequency, and the Planck constant, respectively. (Figure 6b)^{10,22} Compared with the band gap of bulk Cu_{2-x}Se , the larger value resulted from the nano size effect of

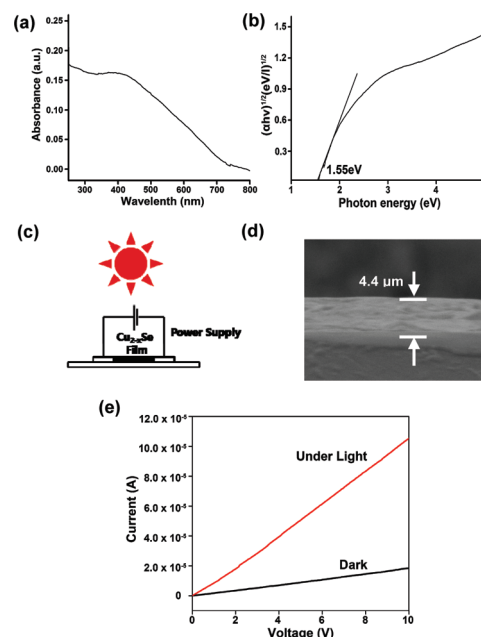


Figure 6. (a) UV/vis absorption spectroscopy; (b) the plot of $(\alpha h\nu)^{1/2} = (1/l)^{1/2} (A h\nu)^{1/2}$ vs $h\nu$, in which α , A , l , ν , and h are absorption coefficient, absorbance, light pathway, frequency, and the Planck constant, respectively; (c) cartoon of setting for photocurrent measurement; (d) SEM image of the prepared Cu_{2-x}Se film; (e) I - V curves of film with and without light from the solar simulator.

materials. Next, the studies on the photoelectronic properties of Cu_{2-x}Se discs were conducted.²¹ (Figure 6c) The film was fabricated on glass using a colloidal solution of materials via drop casting. As shown in Figure 6d, the average film thickness was ca. 4.4 μm . Then, the silver electrode was patterned. The gap and length of the two electrodes were 2 and 3 mm, respectively. The photocurrent was measured using a solar simulator. As shown in Figure 6e, the film showed a promising increase in current by ca. 5.7 times under light, compared to the dark state.²³

In conclusion, high-quality copper selenide nanodiscs with a 2.6 nm thickness were prepared using imidazoline-2-selenone as a new selenium precursor. The phase of prepared nanomaterials was characterized to be cubic Cu_{2-x}Se by HR-TEM, XRPD, EDX and XPS and promising optoelectric properties were observed. We believe that the copper selenide discs in this study can be applied to development of the n/p semiconductor type solar cell devices via a solution-based approach.

Acknowledgment. This work was supported by Grants NRF-2009-0064488 through the National Research Foundation of Korea funded by the Ministry of Education, Science and Technology. H.Y.Y. is thankful for Grants NRF-2009-0094024 (Priority Research Centers Program) and R31-2008-000-10029-0 (WCU program). H.J.K. thanks for Hydrogen Energy R&D Center, a 21st century Frontier R&D Program.

Supporting Information Available: Experimental details, additional TEM images, and ED and XRPD patterns. This material is available free of charge via the Internet at <http://pubs.acs.org>.

(19) See Figure S1 in the Supporting Information.

(20) Wu, Y.; Wadia, C.; Ma, W.; Sadler, B.; Alivisatos, A. P. *Nano Lett.* **2008**, *8*, 2551.

(21) See the Supporting Information for details. (a) Okimura, H.; Matsumae, T. *Thin Solid Films* **1980**, *71*, 53, and references therein. (b) Chen, W. S.; Stewart, J. M.; Mickelson, R. A. *Appl. Phys. Lett.* **1985**, *46*, 1095.

(22) We used the well documented equation, $(\alpha h\nu)^{1/2} = d(h\nu - E_g)$ for indirect transition near the band edge (d and E_g are a constant and band gap energy, respectively).

(23) Class AAA solar simulator (Oriol Co.) was used with 100 mW/cm² power output.